J|A|C|S
ARTICLES
Published on Web 01/09/2007

1,4-Shifts in a Dinuclear Ni(I) Biarylyl Complex: A Mechanistic Study of C−H Bond Activation by Monovalent Nickel

Alana L. Keen, Meghan Doster, and Samuel A. Johnson*

Contribution from the Department of Chemistry & Biochemistry, University of Windsor, Windsor, Ontario, Canada, N9B 3P4

Received October 4, 2006; E-mail: sjohnson@uwindsor.ca

Abstract: The known aryne complex $(PEt_3)_2Ni(\eta^2\text{-}C_6H_2\text{-}4,5\text{-}F_2)$ (**1a**) reacts with a catalytic amount of $Br_2Ni(PEt_3)_2$ over 1% Na/Hg to afford the dinuclear Ni(I) biarylyl complex $[(PEt_3)_2Ni]_2(\mu\text{-}\eta^1\text{:}\eta^1\text{-}3,4\text{-}F_2C_6H_2\text{-}3',4'\text{-}F_2C_6H_2)$ (**2a**), which results from a combination of C−C bond formation and C−H bond rearrangement. The dinuclear benzyne $[(PEt_3)_2Ni]_2(\mu\text{-}\eta^2\text{:}\eta^2\text{-}C_6H_2\text{-}4,5\text{-}F_2)$ (**3**) was obtained by the reaction of **1a** with a stoichiometric amount of $Br_2Ni(PEt_3)_2$ over excess 1% Na/Hg, and **3** was found to catalyze the conversion of **1a** to **2a**. The reaction of **1a** with $B(C_6F_5)_3$ produced the trinuclear complex $(PEt_3)_3Ni_3(\mu_3\text{:}\eta^1\text{:}\eta^1\text{:}\eta^2\text{-}4,5\text{-}F_2C_6H_2)(\mu_3\text{:}\eta^1\text{:}\eta^1\text{:}\eta^2\text{-}4,5\text{-}F_2C_6H_2\text{-}4',5'\text{-}F_2C_6H_2)$ (**6**). The addition of PEt_3 to **6** produced 1 equiv of **1a** and 1 equiv of $[(PEt_3)_2Ni]_2(\mu\text{-}\eta^1\text{:}\eta^1\text{-}4,5\text{-}F_2C_6H_2\text{-}4',5'\text{-}F_2C_6H_2)$ (**7a**). Both **6** and **7a** were identified as intermediates in the conversion of **1a** to **2a**. The analogue $[(PEt_3)(PMe_3)Ni]_2(\mu\text{-}\eta^1\text{:}\eta^1\text{-}4,5\text{-}F_2C_6H_2\text{-}4',5'\text{-}F_2C_6H_2)$ (**7b**) was prepared by the addition of PMe_3 to **6** and was structurally characterized. NMR spectroscopic evidence identified the additional asymmetric biarylyl $[(PEt_3)_2Ni]_2(\mu\text{-}\eta^1\text{:}\eta^1\text{-}4,5\text{-}F_2C_6H_2\text{-}3',4'\text{-}F_2C_6H_2)$ (**8a**) during the conversion of **1a** to **2a**. The initial observation of 2 equiv of **8a** for every equivalent of **2a** produced from solutions of **7a** suggests that **8a** and **2a** are formed from a common intermediate. A crossover labeling experiment shows that the C−H bond rearrangement steps in the conversion of **1a** to **2a** occur with the intermolecular scrambling of hydrogen and deuterium labels. The evidence collected suggests that Ni(I) complexes are capable of activating aromatic C−H bonds.

Introduction

Both stoichiometric and catalytic transformations involving C−H activation are of current interest, due to the synthetic utility that the facile functionalization of unreactive C−H bonds would provide.[1] The relatively low cost of nickel complexes, compared to their more expensive second and third row transition metal counterparts, provides an impetus for their utilization in catalytic or stoichiometric transformations that proceed by C−H bond activation.[2] Unfortunately, calculations have demonstrated that, although the $Ni(PEt_3)_2$ fragment is capable of C−F bond activation,[3] the activation of aromatic C−H bonds by $Ni(PEt_3)_2$ is not thermodynamically favorable.[4] Although a few examples of nickel complexes that perform C−H bond activation have been reported,[5,6] many of these involve C−H bonds rendered more reactive by adjacent substituents.

We recently communicated the isomerization of the aryne complex $(PEt_3)_2Ni(\eta^2\text{-}C_6H_2\text{-}4,5\text{-}F_2)$ (**1a**) to the dinuclear Ni(I) complex $[(PEt_3)_2Ni]_2[\mu\text{-}\eta^1\text{:}\eta^1\text{-}(C_6H_2\text{-}3,4\text{-}F_2)]_2$ (**2a**) when treated with $Br_2Ni(PEt_3)_2$ over 1% Na/Hg, as shown in Scheme 1.[7] Two possible mechanistic pathways were proposed, one in which C−H bond activation precedes C−C bond formation, and a second where C−C bond formation occurs first, and the resultant biarylyl complex undergoes isomerization by C−H bond activation. These two mechanistic manifolds are shown in Scheme 1 as mechanisms A and B. In each reaction step, multiple elementary processes could be involved.

The involvement of d^9 Ni(I) intermediates in C−H bond activation, which is implied in mechanism B, would render this C−H bond activation unique compared to those that rely on second and third row transition metal complexes with d^6 and d^8 electronic configurations. Only a few related organometallic dinuclear Ni(I) complexes are known,[8,9] although their reported

(1) (a) Labinger, J. A.; Bercaw, J. E. *Nature* **2002**, *417*, 507−514. (b) Arndtsen, B. A.; Bergman, R. G.; Mobley, T. A.; Peterson, T. H. *Acc. Chem. Res.* **1995**, *28*, 154−162. (c) Crabtree, R. H. *J. Chem. Soc., Dalton Trans.* **2001**, 2437−2450. (d) Crabtree, R. H. *J. Organomet. Chem.* **2004**, *689*, 4083−4091. (e) Lersch, M.; Tilset, M. *Chem. Rev.* **2005**, *105*, 2471−2526. (f) Shilov, A. E.; Shul'pin, G. B. *Chem. Rev.* **1997**, *97*, 2879−2932. (g) Kakiuchi, F.; Murai, S. *Acc. Chem. Res.* **2002**, *35*, 826−834. (h) Godula, K.; Sames, D. *Science* **2006**, *312*, 67−72.
(2) Jolly, P. W.; Wilke, G. *The Organic Chemistry of Nickel*; Organometallic Chemistry Series; Academic Press: New York, 1974; Vol. 1.
(3) (a) Braun, T.; Foxon, S. P.; Perutz, R. N.; Walton, P. H. *Angew. Chem., Int. Ed.* **1999**, *38*, 3326−3329. (b) Braun, T.; Cronin, L.; Higgitt, C. L.; McGrady, J. E.; Perutz, R. N.; Reinhold, M. *New J. Chem.* **2001**, *25*, 19−21. (c) Bach, I.; Poerschke, K.-R.; Goddard, R.; Kopiske, C.; Krueger, C.; Rufinska, A.; Seevogel, K. *Organometallics* **1996**, *15*, 4959−4966.
(4) Reinhold, M.; McGrady, J. E.; Perutz, R. N. *J. Am. Chem. Soc.* **2004**, *126*, 5268−5276.
(5) (a) Nakao, Y.; Kanyiva, K. S.; Oda, S.; Hiyama, T. *J. Am. Chem. Soc.* **2006**, *128*, 8146−8147. (b) Kleiman, J. P.; Dubeck, M. *J. Am. Chem. Soc.* **1963**, *85*, 1544−1545. (c) Tsuda, T.; Kiyoi, T.; Saegusa, T. *J. Org. Chem.* **1990**, *55*, 2554−2558. (d) Brunkan, N. M.; Brestensky, D. M.; Jones, W. D. *J. Am. Chem. Soc.* **2004**, *126*, 3627−3641. (e) Clement, N. D.; Cavell, K. J. *Angew. Chem., Int. Ed.* **2004**, *43*, 3845−3847. (f) Clement, N. D.; Cavell, K. J.; Jones, C.; Elsevier, C. J. *Angew. Chem., Int. Ed.* **2004**, *43*, 1277−1279. (g) Ogoshi, S.; Ueta, M.; Oka, M.-A.; Kurosawa, H. *Chem. Commun.* **2004**, 2732−2733. (h) Brunkan, N. M.; Brestensky, D. M.; Jones, W. D. *J. Am. Chem. Soc.* **2004**, *126*, 3627−3641. (i) van der Boom, M. E.; Liou, S.-Y.; Shimon, L. J. W.; Ben-David, Y.; Milstein, D. *Inorg. Chim. Acta* **2004**, *357*, 4015−4023.
(6) Vicic, D. A.; Jones, W. D. *J. Am. Chem. Soc.* **1999**, *121*, 7606−7617.
(7) Keen, A. L.; Johnson, S. A. *J. Am. Chem. Soc.* **2006**, *128*, 1806−1807.

10.1021/ja067112w CCC: $37.00

Scheme 1

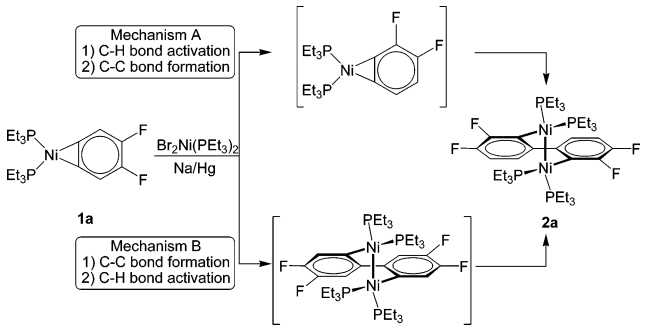

reactivities include reversible C−C bond activation.[10] The activation of C−H bonds at room temperature by Ni(I) complexes could provide a new economically viable methodology for syntheses involving C−H bond activation. The study provides full experimental details for the conversion of **1a** to **2a** and a mechanistic study that provides insight into the nature of the Ni-mediated C−H bond activation step.

Results and Discussion

The alkali metal reduction of $(PEt_3)_2NiBr(2\text{-}Br\text{-}4,5\text{-}F_2C_6H_2)$ in hydrocarbon solvents to form the aryne complex **1a** is a known reaction;[11] however, in our hands, no reduction took place within 24 h when the starting material, $(PEt_3)_2NiBr(2\text{-}Br\text{-}4,5\text{-}F_2C_6H_2)$, was rigorously purified. The addition of catalysts such as $BrNi(PEt_3)_3$ and $Br_2Ni(PEt_3)_2$ allows this reduction to proceed with Na/Hg in 4 h to produce **1a**; however, when $Br_2Ni(PEt_3)_2$ was utilized the reaction continues, and the conversion of **1a** to the dinuclear Ni(I) complex **2a**, shown in Scheme 1, was observed after 1−2 days. Complex **2a** can also be prepared using isolated **1a** in the presence of Na/Hg and catalytic $Br_2Ni(PEt_3)_2$.

An ORTEP depiction of the solid-state molecular structure of **2a** is shown in Figure 1. The structure demonstrates that **2a** is a dinuclear Ni(I) complex, with a Ni−Ni bond distance of 2.3710(5) Å and approximate C_2 symmetry. The biarylyl fragment bridges two $Ni(PEt_3)_2$ fragments in a μ-η^1:η^1 manner, with a C(1)−C(6)−C(7)−C(8) torsion angle of 30.8(6)°. This is an unusual bonding mode for a biarylyl ligand bridging a metal−metal bond.[12,13] Complex **2a** displays Ni(1)−C(1) and Ni(2)−C(8) bond lengths of 1.965(3) and 1.952(3) Å, as well as longer Ni(1)−C(8) and Ni(2)−C(1) distances of 2.317(3) and 2.308(3) Å. Neither Ni atom lies in a plane with either of the aryl rings, possibly because these longer Ni−C distances are weak bonding interactions, not simply short contacts. Excluding the Ni(1)−C(8) and N(2)−C(1) interactions, the geometries at the Ni centers are distorted square planar. The donors associated with P(1) and P(4) are approximately trans to the Ni−Ni bond, whereas the donors associated with P(2) and P(3) are approximately trans to the shorter Ni−C bonds. The longer Ni(1)−C(8) and Ni(2)−C(1) interactions are directed toward the Ni centers at an approximately 45° angle to the planes described by the other four attached atoms.

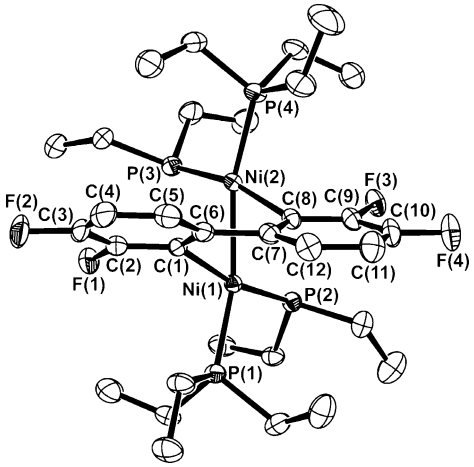

Figure 1. Solid-state molecular structure of **2a** as determined by X-ray crystallography. Hydrogen atoms and two ethyl substituents, associated with P(2) and P(3), are omitted for clarity. Selected bond lengths (Å), angles (deg), and dihedral angles (deg): Ni(1)−Ni(2), 2.3710(5); Ni(1)−C(1), 1.965(3); Ni(2)−C(1), 2.308(3); Ni(1)−P(1), 2.2091(8); Ni(1)−P(2), 2.2232(8); P(1)−Ni(1)−Ni(2), 157.72(3); P(2)−Ni(1)−Ni(2), 103.25(2); C(1)−Ni(1)−Ni(2), 63.50(7); C(1)−Ni(1)−P(1), 94.98(8); C(1)−C(6)−C(7), 112.7(2); C(1)−C(6)−C(7)−C(8), 30.8(6).

The 213 K $^{31}P\{^1H\}$ NMR spectrum contains two ^{31}P environments, consistent with the C_2 symmetry observed in the solid state. One of these is a virtual triplet with a J_{PP} value of 5.4 Hz. To account for the strong coupling between chemically equivalent phosphorus nuclei that is mandatory for virtual coupling to occur, a Ni−Ni bond must be present. The second ^{31}P environment can be modeled as a virtual triplet of doublets of doublets, due to coupling to ^{31}P as well as both ^{19}F environments (J_{PP} = 5.4 Hz, J_{PF} = 7.1 Hz, J_{PF} = 11.3 Hz).

As the sample is warmed, the ^1H and ^{31}P NMR signals associated with the PEt_3 groups begin to broaden. The barrier to this process is estimated to be 23 kJ/mol from the ^1H and $^{31}P\{^1H\}$ NMR data prior to coalescence; however, at near 323 K the sample decomposes rapidly. Thus, although it is apparent that the phosphorus environments can exchange rapidly at higher temperatures, the mechanism of this rearrangement is not clear.

Synthesis of a μ-η^2:η^2 Aryne Complex. The slow conversion of **1a** to **2a** allowed for the observation of several long-lived intermediates by ^1H, $^{31}P\{^1H\}$, and ^{19}F NMR spectroscopy, and the reaction of a pentane solution of **1a** with 1 equiv of $Br_2Ni(PEt_3)_2$ and excess Na/Hg, as shown in eq 1, allowed for the isolation of orange crystals of one of these species, $[(PEt_3)_2Ni]_2(\mu\text{-}\eta^2\text{:}\eta^2\text{-}C_6H_2F_2)$ (**3**). Complex **3** exhibits a virtual triplet in the aromatic region of the ^1H NMR spectrum, similar to that of **1a**. The ^{19}F NMR spectrum contains a single environment at δ −74.0, which is a virtual triplet of pentets due to coupling to the aromatic protons and a 2.3 Hz $^5J_{PF}$ to four chemically equivalent ^{31}P environments.

The solid-state structure of **3** was determined by X-ray crystallography and is shown in Figure 2. The aryne fragment bridges two $Ni(PEt_2)_2$ fragments in a μ-η^2:η^2 bonding mode.

(8) Eisch, J. J.; Piotrowski, A. M.; Han, K. I.; Kruger, C.; Tsay, Y. H. *Organometallics* **1985**, *4*, 224−231.
(9) Diercks, R.; Stamp, L.; Kopf, J.; Heindirk, T. D. *Angew. Chem.* **1984**, *96*, 891−895.
(10) Ramakrishna, T. V. V.; Sharp, P. R. *Organometallics* **2004**, *23*, 3079−3081.
(11) Bennett, M. A.; Wenger, E. *Organometallics* **1995**, *14*, 1267−1277.
(12) (a) Perthuisot, C.; Edelbach, B. L.; Zubris, D. L.; Jones, W. D. *Organometallics* **1997**, *16*, 2016−2023. (b) Leong, W. K.; Chen, G. *Organometallics* **2001**, *20*, 2280−2287. (c) Leong, W. K.; Chen, G. *Organometallics* **2001**, *20*, 5771−5773. (d) Chehata, A.; Oviedo, A.; Arevalo, A.; Bernes, S.; Garcia, J. J. *Organometallics* **2003**, *22*, 1585−1587. (e) Yeh, W.-Y.; Hsu, S. C. N.; Peng, S.-M.; Lee, G.-H. *Organometallics* **1998**, *17*, 2477−2483. (f) Mueller, J.; Haensch, C.; Pickardt, J. *J. Organomet. Chem.* **1983**, *259*, C21−C25.
(13) Bennett, M. A.; Griffiths, K. D.; Okano, T.; Parthasarathi, V.; Robertson, G. B. *J. Am. Chem. Soc.* **1990**, *112*, 7047−7048.

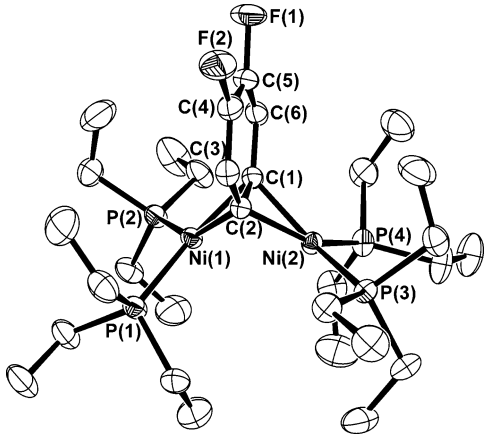

Figure 2. Solid-state molecular structure of **3** as determined by X-ray crystallography. Hydrogen atoms are omitted for clarity. Selected bond lengths (Å), angles (deg), and dihedral angles (deg): Ni(1)···Ni(2), 2.7242(5); Ni(1)−C(1), 1.916(2); Ni(1)−C(2), 1.962(2); Ni(2)−C(2), 1.920(2); Ni(2)−C(1), 1.963(2); Ni(1)−P(1), 2.1664(7); Ni(1)−P(2), 2.1572(7); C(1)−C(2), 1.390(3); C(2)−C(3), 1.427(3); C(3)−C(4), 1.353(3); C(4)−C(5), 1.405(4); C(5)−C(6), 1.356(4); C(6)−C(1), 1.420(3); P(2)−Ni(1)−P(1), 109.80(3).

This bonding mode has been observed before with nickel alkyne complexes[14] but is unique for aryne complexes. More typically, aryne moieties bridging two metal centers adopt a μ-η^1:η^1 bonding mode, which is best described as a 1,2-disubstituted phenylene.[15] In complex **3**, the C(1)−C(2) distance of 1.390(3) Å is typical for an aromatic C−C bond, but the remainder of the aryne ring shows bond length alternations due to backbonding to the aromatic π-system. The Ni(1)−Ni(2) distance of 2.7242(3) Å in **3** is 0.3532(6) Å longer than the Ni−Ni bond in **2a**, which indicates that no significant Ni−Ni bond is present in this complex. The geometries around the nickel centers are slightly distorted from planar, with the $Ni(PEt_3)_2$ groups twisted slightly with respect to each other, as can be seen from the P(1)−Ni(1)−Ni(2)−P(3) torsion angle of −159.5(3)°. As a result, the aryne moiety does not bridge perfectly symmetrically, and the Ni(1)−C(1) and Ni(2)−C(2) distances are slightly shorter than the Ni(1)−C(2) and Ni(2)−C(1) distances. Related arene π-adducts have been observed as intermediates for C−F bond cleavage,[3] but no C−F bond activation occurs in these complexes.

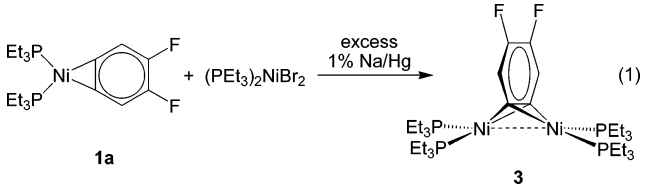

Pure solutions of complex **3** do not convert cleanly into **2a**, but the addition of small amounts of **3** to solutions of **1a** does catalyze this conversion; thus, Hg does not appear to be involved directly in either the C−C bond forming or C−H activation steps.[16] Using ^{19}F NMR spectroscopy, we could observe a second intermediate during these reactions. Similar to complex **3**, this intermediate also appears early in the reaction but has two fluorine environments in the ^{19}F NMR spectrum. Both mechanisms from Scheme 1 have intermediates that should exhibit two ^{19}F environments, and thus attempts were made to synthesize these complexes or related analogues to determine which pathway operates.

Scheme 2

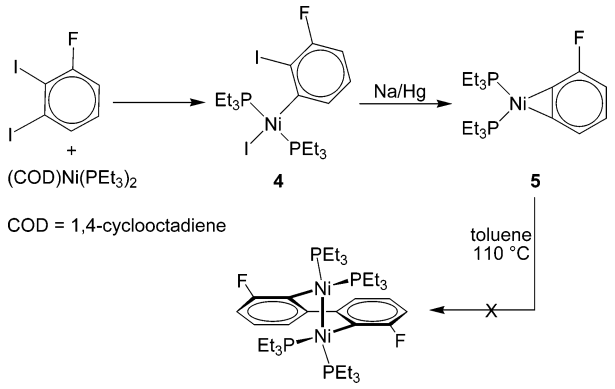

Synthesis of a 3-Fluoroaryne Complex. There is no efficient synthetic route to the speculative aryne complex intermediate of mechanism A in Scheme 1, $(PEt_3)_2Ni(\eta^2\text{-}3,4\text{-}F_2C_6H_2)$; however, the question of whether the location of the fluoro substituents on the aryne fragment can promote the dinuclear coupling of aryne complexes, as suggested in the second step of mechanism A of Scheme 1, can be addressed by synthesizing a related aryne complex bearing a fluoro-substituent in the 3-position. The oxidative addition of 1-fluoro-2,3-diodobenzene[17] to $(COD)Ni(PEt_3)_2$ was regioselective and produced a single isomer, $(PEt_3)_2NiI(3\text{-}F\text{-}2\text{-}I\text{-}C_6H_3)$ (**4**) as shown in Scheme 2. The connectivity was determined by X-ray crystallography, and an ORTEP depiction of this structure is provided in the Supporting Information. The reduction of this product over Na/Hg was rapid and produced the aryne complex $(PEt_3)_2Ni(\eta^2\text{-}3\text{-}F\text{-}C_6H_3)$ (**5**). Unfortunately, this product is a low-melting oil; similar behavior has been noted for the closely related complex $(PEt_3)_2Ni(\eta^2\text{-}C_6H_4)$.[11] The ^{31}P{^{1}H} NMR spectrum of the pure product displays two signals; however, with the slightest impurity of PEt_3 a single resonance is observed. Attempts to promote the dinuclear coupling of this aryne complex failed. The complex is thermally stable for days in refluxing toluene, and thus it seems unlikely that the intermediate in mechanism B of Scheme 1 would spontaneously couple in preference to **1a**.

Coupling of Arynes. It is plausible that the $Ni(PEt_3)_2$ fragment could behave as a Lewis acid and abstract PEt_3 from **1a** to form an unstable $(PEt_3)Ni(C_6H_2\text{-}4,5\text{-}F_2)$ moiety, which could then dimerize and undergo C−C bond formation to form a precursor to **2a**. In an attempt to mimic this reaction sequence with a reagent that would react strictly as a Lewis acid, we added 1 equiv of $B(C_6F_5)_3$ to a pentane solution of **1a**, as shown in eq 2. This reaction produced the white precipitate $Et_3P{\cdot}B(C_6F_5)_3$ and a brown solution. Cooling the brown pentane solution to

(14) Day, V. W.; Abdel-Meguid, S. S.; Dabestani, S.; Thomas, M. G.; Pretzer, W. R.; Muetterties, E. L. *J. Am. Chem. Soc.* **1976**, *98*, 8289−8291.
(15) (a) Retboll, M.; Edwards, A. J.; Rae, A. D.; Willis, A. C.; Bennett, M. A.; Wenger, E. *J. Am. Chem. Soc.* **2002**, *124*, 8348−8360. (b) Bennett, M. J.; Graham, W. A. G.; Stewart, R. P., Jr.; Tuggle, R. M. *Inorg. Chem.* **1973**, *12*, 2944−2949. (c) Rausch, M. D.; Gastinger, R. G.; Gardner, S. A.; Brown, R. K.; Wood, J. S. *J. Am. Chem. Soc.* **1977**, *99*, 7870−7876. (d) Grushin, V. V.; Vymenits, A. B.; Yanovskii, A. I.; Struchkov, Y. T.; Vol'pin, M. E. *Organometallics* **1991**, *10*, 48−49. (e) Bennett, M. A.; Schwemlein, H. P. *Angew. Chem.* **1989**, *101*, 1349−1373. (f) Jones, W. M.; Klosin, J. *Adv. Organomet. Chem.* **1998**, *42*, 147−221. (g) Bennett, M. A.; Wenger, E. *Chem. Ber.* **1997**, *130*, 1029−1042. (h) Cullen, W. R.; Rettig, S. J.; Zhang, H. *Organometallics* **1993**, *12*, 1964−1968.
(16) Begum, R. A.; Sharp, P. R. *Organometallics* **2005**, *24*, 2670−2678.
(17) Rausis, T.; Schlosser, M. *Eur. J. Org. Chem.* **2002**, *19*, 3351−3358.

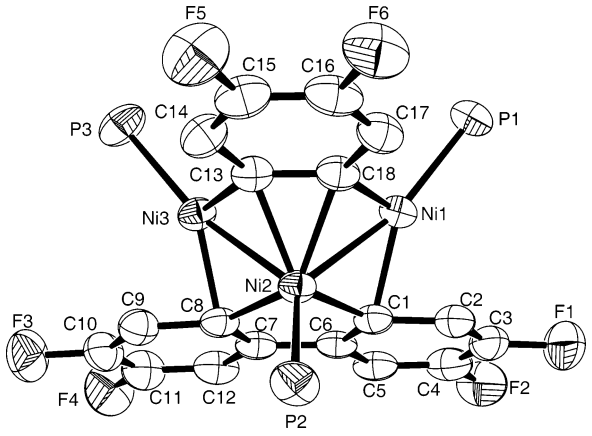

Figure 3. Solid-state molecular structure of **6** as determined by X-ray crystallography. Ethyl substituents on the phosphine ligands and hydrogen atoms are omitted for clarity. Selected bond lengths (Å), angles (deg), and dihedral angles (deg): Ni(1)−Ni(2), 2.3798(6); Ni(1)−C(1), 1.962(3); Ni(2)−C(1), 1.974(3); Ni(1)−P(1), 2.1685(1); P(1)−Ni(1)−Ni(2), 161.16(3); P(2)−Ni(2)−Ni(1), 132.88(3); C(1)−Ni(1)−Ni(2), 53.03(9); C(1)−Ni(1)−P(1), 145.79(9); C(1)−C(6)−C(7), 115.5(3). Dihedral angles (deg) C(1)−C(6)−C(7)−C(8), 30.9(6).

−40 °C provided $[(PEt_3)Ni]_3(\mu_3\text{-}4,5\text{-}F_2C_6H_2)(\mu_3\text{-}4,5\text{-}F_2C_6H_2\text{-}4',5'\text{-}F_2C_6H_2)$ (**6**) as dark brown crystals.

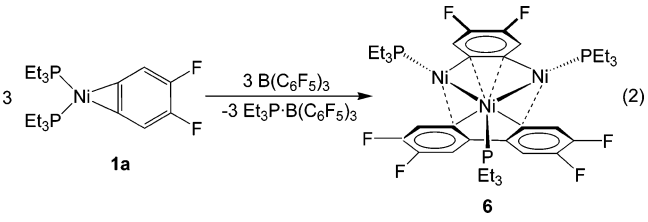

An ORTEP representation of the solid-state molecular structure of trinuclear complex **6** is shown in Figure 3. The complex is composed of one uncoupled 4,5-$F_2C_6H_2$-aryne unit and a biarylyl unit with the fluorine substituents in the positions expected in the absence of C−H bond activation. Open trinuclear nickel clusters are not common,[18] although a related compound has been reported as a minor byproduct from the reduction of $NiCl(2\text{-}ClC_6H_4)(P^iPr_3)_2$ with 1% sodium amalgam.[13]

When relatively large catalyst loadings of $(PEt_3)_2NiBr_2$ over Na/Hg are used in the conversion of **1a** to **2a**, the presence of complex **6** is ascertained by ^{19}F NMR spectroscopy, and under these conditions **6** is found to slowly convert to **2a**. Density functional theory (DFT) calculations on model complexes where the PEt_3 ligands are replaced by PMe_3 donors predict that the formation of the biarylyl intermediate from Scheme 1, $[(PEt_3)_2Ni]_2(3,4\text{-}F_2C_6H_2\text{-}3',4'\text{-}F_2C_6H_2)$, from **1a** should be both substantially exothermic ($\Delta H = -33$ kcal/mol) and thermodynamically favorable, unlike in some similar systems, where C−C coupling is nearly thermoneutral.[10] One plausible role of the catalytic $Ni(PEt_3)_2$ moiety in the conversion of **1a** to **2a** is as a Lewis acid capable of abstracting a PEt_3 ligand, which provides a low activation energy pathway for the coupling of two aryne complexes.

Synthesis of Biarylyl Intermediates. Complex **6** can be used as a precursor to the intermediate postulated for mechanism B shown in Scheme 1. The addition of PEt_3 to the trinuclear complex **6** provided the dinuclear complex $[(PEt_3)_2Ni]_2(3,4\text{-}F_2C_6H_2\text{-}3',4'\text{-}F_2C_6H_2)$ (**7a**), along with 1 equiv of **1a**, as shown in Scheme 3. As monitored by ^1H, $^{31}P\{^1H\}$, and ^{19}F NMR spectroscopy, the reaction of **6** with PEt_3 is relatively slow. Complex **7a** exhibits two ^{31}P resonances at δ 8.1 and −6.6, similar to **2a**, as well as two ^{19}F environments, and two aromatic ^1H environments. A comparison of the NMR parameters of this complex with the intermediate observed almost immediately after the addition of a source of $Ni(PEt_3)_2$ to **1a** allowed us to assign this intermediate as **7a**, which confirms that mechanism B in Scheme 1 operates in the conversion of **1a** to **2a**.

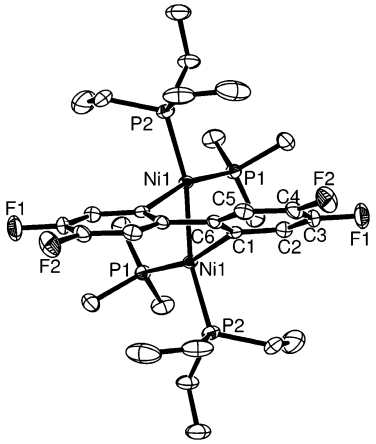

Figure 4. Solid-state molecular structure of **7b** as determined by X-ray crystallography. Hydrogen atoms are omitted for clarity. Selected bond lengths (Å): Ni(1)−C(1), 1.959(3) and 2.346(3); Ni(1)−P(1), 2.1823(10); Ni(1)−P(2), 2.1928(10); Ni(1)−Ni(1), 2.3079(8).

Unfortunately, compound **7a** is too thermally unstable to be isolated as a pure compound, and the equivalent of **1a** produced from the reaction that forms **7a** cannot be separated by recrystallization. In the absence of excess phosphine, **7a** is thermally unstable and converts to **2a** over the course of ∼48 h at room temperature. This occurs without the addition of any catalyst, though trace amounts of $Ni(PEt_3)_4$ were difficult to remove.

The addition of PMe_3 in lieu of PEt_3 to a pentane solution of **6** provided an isolable analogue to **7a**, as shown in Scheme 3. The aryne complex byproduct, $(PMe_3)(PEt_3)Ni(\eta^2\text{-}4,5\text{-}F_2C_6H_2)$ (**1b**), is considerably less soluble than the dinuclear product, $[(PEt_3)(PMe_3)Ni]_2(3,4\text{-}F_2C_6H_2\text{-}3',4'\text{-}F_2C_6H_2)$ (**7b**), and precipitates from pentane as a yellow solid. The resultant brown pentane solution can then be concentrated and cooled to −40 °C to provide X-ray quality crystals of **7b**. The ^{19}F NMR spectrum and aromatic region of the ^1H NMR spectrum of **7b** are nearly identical to that of **7a**, and the $^{31}P\{^1H\}$ NMR spectrum exhibits two phosphorus environments.

The solid-state molecular structure of **7b** is shown in Figure 4 and has crystallographically imposed C_2 symmetry. The complex is similar to **2a**, in that a biarylyl ligand is bridged by two Ni(I) moieties. Unlike **2a**, the fluorine substituents are in the 4,5 and 4′,5′ positions of the biarylyl fragment. The bulkier PEt_3 groups occupy the sites trans to the Ni−Ni bond, whereas the smaller PMe_3 donors are adjacent to each other and trans to the Ni(1)−C(1) bonds. The Ni−Ni bond in **7b** is 0.0631(9) Å shorter than the Ni−Ni bond in **2**, likely due to the lesser steric bulk of PMe_3 relative to that of PEt_3.

(18) Pasynkiewicz, S.; Pietrzykowski, A.; Kryza-Niemiec, B.; Zachara, J. *J. Organomet. Chem.* **1998**, *566*, 217−224.

Scheme 3

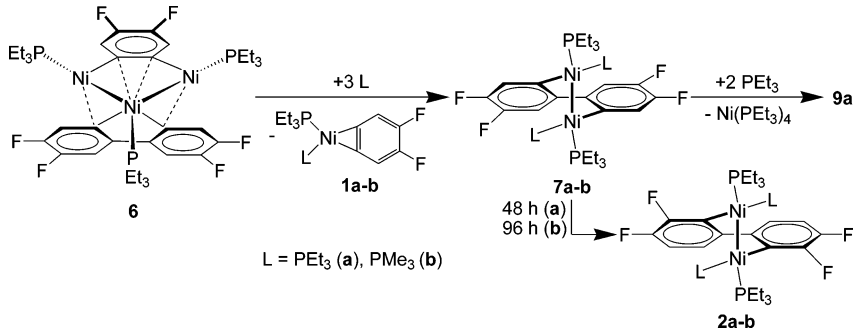

Scheme 4

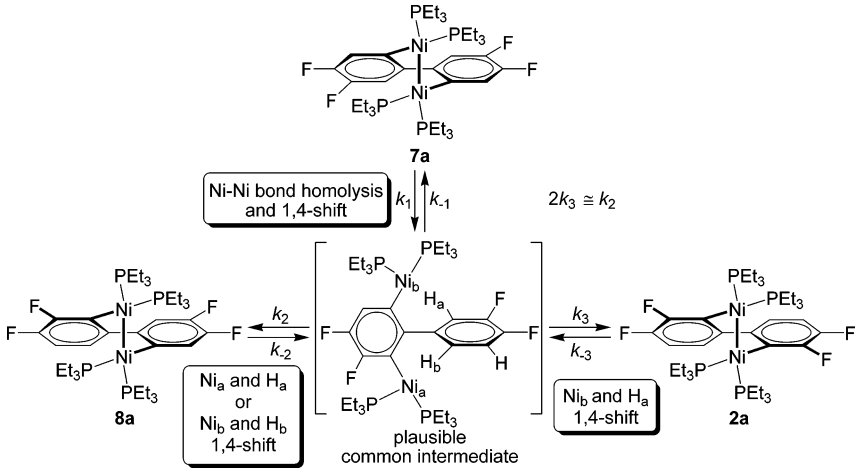

Similar to those of **7a**, solutions of **7b** are thermally unstable but convert much slower, over the course of 4 days, to an analogue of **2a**, $[(PEt_3)(PMe_3)Ni]_2(3,4\text{-}F_2C_6H_2\text{-}3',4'\text{-}F_2C_6H_2)$ (**2b**). Complex **2b** has ^{19}F and ^1H NMR spectra that are nearly identical to those of **2a**. The $^{31}P\{^1H\}$ NMR spectrum has a virtual triplet at δ −0.52, which is assigned as the PEt_3 donor, and a multiplet at δ −20.2, which can be ascribed to the PMe_3 donor.

These alternate routes to intermediate **7a** and its analogue **7b** allowed for the identification of another intermediate in the conversion of **1a** to **2a**. For both the thermal conversion of **7a** to **2a** and the conversion of **7b** to **2b**, intermediates are observed that exhibit four ^{19}F resonances of equal intensity, a pair of which have chemical shifts similar to those of **7a**, and a pair of which have chemical shifts similar to those of **2a**. During the isomerization of **7b**, it was possible to characterize this asymmetric intermediate by a combination of ^{19}F and $^{31}P\{^1H\}$ NMR spectroscopy. The $^{31}P\{^1H\}$ NMR spectra exhibit four $^{31}P\{^1H\}$ resonances. Two ^{31}P resonances at δ 0.4 and −1.0 are associated with the PEt_3 moieties and are coupled to each other with a $^3J_{PP}$ value of 97 Hz. Both resonances also exhibit $^2J_{PP}$ values of 15.0 and 15.3 Hz, respectively, due to coupling with cis-disposed PMe_3 groups, and the resonance at δ −1.0 has an additional poorly resolved $^4J_{PF}$ value of approximately 5 Hz. The ^{31}P resonances associated with the PMe_3 moieties are a multiplet at δ −19.5 and a doublet at δ −20.3 with $^2J_{PP} = 15.0$ Hz. This intermediate is assigned as the asymmetric complex $[(PEt_3)(PMe_3)Ni]_2(\mu\text{-}\eta^1\text{:}\eta^1\text{-}3,4\text{-}F_2C_6H_2\text{-}4',5'\text{-}F_2C_6H_2)$ (**8b**), and the analogous intermediate observed in the conversion of **7a** to **2a** can be assigned as $[(PEt_3)_2Ni]_2(\mu\text{-}\eta^1\text{:}\eta^1\text{-}3,4\text{-}F_2C_6H_2\text{-}4',5'\text{-}F_2C_6H_2)$ (**8a**). These intermediates are always present as mixtures with complexes of similar solubility and thus cannot be isolated.

Comparison of the concentrations of **8a** and **2a**, as determined by peak integrals in the ^{19}F NMR spectrum, demonstrated that at the start of the isomerization of **7a** the asymmetric species **8a** and the final product **2a** are produced in a 2:1 ratio, respectively. This implies that a common intermediate exists that forms **8a** twice as rapidly as it forms **2a**. The immediate appearance of **2a** also reveals that although **8a** can be converted to **2a**, it is not directly on the reaction pathway from **7a**. A similar result is seen for the isomerization of **7b**.

Any postulated mechanism for the conversion of **7a**,**b** to **2a**,**b** must explain this initial 2:1 ratio of **8a**,**b** to **2a**,**b**, which eliminates many possible reaction pathways. The isomerization of **7a** to **2a** requires the migration of the hydrogen substituents in the ortho (6 and 6′) positions of the biarylyl ligand. It can be speculated that the Ni−Ni bond reversibly homolytically cleaves to give a binuclear Ni(I) complex with *ortho*-C−H agostic interactions that result in a four-coordinate environment about the Ni(I) centers. These agostic interactions could aid in the activation of the *ortho*-C−H bonds, although there is precedent for stable three-coordinate Ni(I) complexes.[19] The increased rate of rearrangement observed for **7a** compared to that of **7b** can be explained by the increased steric interactions of the adjacent PEt_3 group on opposing metal centers decreasing the barrier to

(19) (a) Bradley, D. C.; Hursthouse, M. B.; Smallwood, R. J.; Welch, A. J. *Chem. Commun.* **1972**, 872. (b) Eaborn, C.; Hill, M. S.; Hitchcock, P. B.; Smith, J. D. *Chem. Commun.* **2000**, 691−692. (c) Kitiachvili, K. D.; Mindiola, D. J.; Hillhouse, G. L. *J. Am. Chem. Soc.* **2004**, *126*, 10554−10555. (d) Bai, G.; Wei, P.; Das, A. K.; Stephan, D. W. *J. Chem. Soc., Dalton Trans.* **2006**, 1141−1146. (e) Bai, G.; Wei, P.; Stephan, D. W. *Organometallics* **2005**, *24*, 5901−5908. (f) Melenkivitz, R.; Mindiola, D. J.; Hillhouse, G. L. *J. Am. Chem. Soc.* **2002**, *124*, 3846−3847.

Ni−Ni bond homolysis. A plausible common intermediate for complexes **8a** and **2a** could be obtained from Ni−Ni bond homolysis, followed by a 1,4-shift[20−23] of the $Ni_a(PEt_3)_2$ moiety, as shown in Scheme 4. Such an intermediate could convert to **8a** by an additional 1,4-shift that exchanged Ni_a and H_a or via a 1,4-shift that exchanged the locations of Ni_b and H_b. The conversion to **2a** could only occur via the postulated common intermediate undergoing a 1,4-shift that exchanged the locations of Ni_b and H_a. The only other possible 1,4-shift, which exchanges Ni_a and H_b, simply regenerates **7a**. If the enthalpic barriers for these rates are approximately equal, the two permutations by which **8a** can be formed from the intermediate would result in the value of the rate constant k_2 being twice the value of k_3 shown in Scheme 4, despite approximately equal activation energies. That the enthalpic barriers should be similar is reasonable, since this is likely a relatively high-energy intermediate, and the conversions to **2a**, **7a**, and **8a** should all be exothermic and have early transition states.

Initially, complex **2a** forms rapidly from **7a** at room temperature, and appreciable conversions to **2a** and **8a** are observed after 15 min. The rate at which **2a** is produced slows as **7a** is consumed. The 2 equiv of **8a** formed then take much longer to convert to **2a**. It is known that the presence of proximal electron-withdrawing groups stabilize late transition metal−carbon bonds,[24] and DFT calculations show that the model complex for **2a**, $[(PMe_3)_2Ni]_2(\mu\text{-}\eta^1\text{:}\eta^1\text{-}3,4\text{-}F_2C_6H_2\text{-}3',4'\text{-}F_2C_6H_2)$, is predicted to be 10.8 kcal/mol more stable than the model complex for **7a**, $[(PMe_3)_2Ni]_2(\mu\text{-}\eta^1\text{:}\eta^1\text{-}4,5\text{-}F_2C_6H_2\text{-}4',5'\text{-}F_2C_6H_2)$. DFT calculations therefore predict that complex **8a** should be approximately 5.4 kcal/mol more stable than **7a**. If one presumes that the activation energies for the reactions associated with the rate constants k_1, k_2, and k_3 are approximately equal, as evidenced from the observation of 2 equiv of **8a** for every equivalent of **2a** produced early in the reaction, then the rate constant k_{-2} should be approximately 2 to 3 orders of magnitude smaller than k_{-1}, due to an approximately 5 kcal/mol larger activation energy for this reaction. This result is consistent with the rapid formation of **2a** and **8a** from **7a**, as well as the observation that reaction times of approximately 48 h are needed for the complete conversion of **8a** to **2a**. These results also predict that the rate constant k_{-3} is so small that this reverse reaction occurs to a negligible degree under the experimental conditions used.

Evidence against Mononuclear Biarylyls as Intermediates. Alternate pathways to C−H bond activation that do not require the involvement of Ni(I) in the C−H bond activation steps were also considered. In the presence of excess phosphine, **7a** converts cleanly into a new product, **9a**, which displays two ^1H environments, two ^{19}F environments, a single ^{31}P environment, and J_{FH} values consistent with no change in the substitution pattern of the biarylyl ligand. Complex **9a** could not be isolated because it is thermally unstable and decomposes in the absence of PEt_3 to a variety of unidentified compounds, none of which are complex **2a**. The observation of $Ni(PEt_3)_4$ by $^{31}P\{^1H\}$ NMR spectroscopy as a byproduct in the conversion of **7a** to **9a** in excess PEt_3 leads us to believe that this compound is the mononuclear species $(PEt_3)_2Ni(3,4\text{-}F_2C_6H_2\text{-}3',4'\text{-}F_2C_6H_2)$, derived from the loss of $Ni(PEt_3)_2$ from **7a** as $Ni(PEt_3)_4$. The related mononuclear biarylyl complex $(PEt_3)_2Ni(\eta^2\text{-}C_6H_4C_6H_4)$ is known to be thermally unstable in the absence of excess phosphine.[8] DFT calculations revealed that the reaction of the model compound $(PMe_3)_2Ni(\mu\text{-}\eta^1\text{:}\eta^1\text{-}4,5\text{-}F_2C_6H_2\text{-}4',5'\text{-}F_2C_6H_2)$ with 2 equiv of PMe_3 to provide $Ni(PMe_3)_4$ and $(PMe_3)_2Ni(\eta^2\text{-}4,5\text{-}F_2C_6H_2\text{-}4',5'\text{-}F_2C_6H_2)$ should occur with only a slightly exothermic ΔH of −7.6 kcal/mol and a slightly unfavorable ΔG°_{298} of 4.8 kcal/mol. The small value of ΔG°_{298} indicates that the conversion of **7a** to **9a** could be thermodynamically viable in the presence of excess phosphine. A similar calculation with an analogue of **2a**, $(PMe_3)_2Ni(\eta^2\text{-}3,4\text{-}F_2C_6H_2\text{-}3',4'\text{-}F_2C_6H_2)$, demonstrated that this complex is 2 kcal/mol more stable with respect to this disproportionation reaction. Although we could not isolate and crystallize **9a**, the DFT calculations on the model complex predict a structure distorted between square planar and tetrahedral, which is an unusual geometry for a nickel(II) complex bearing strong-field ligands. For comparison, the solid-

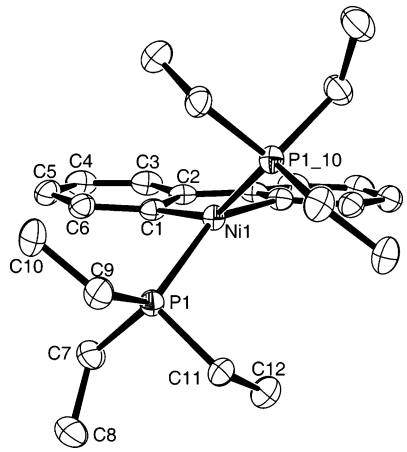

Figure 5. Solid-state molecular structure of **10** as determined by X-ray crystallography. Hydrogen atoms are omitted for clarity. Selected bond lengths (Å), angles (deg), and dihedral angles (deg): Ni(1)−C(1), 1.971-(5); Ni(1)−P(1), 2.236(7); C(1)−Ni(1)−P(1), 96.99(6).

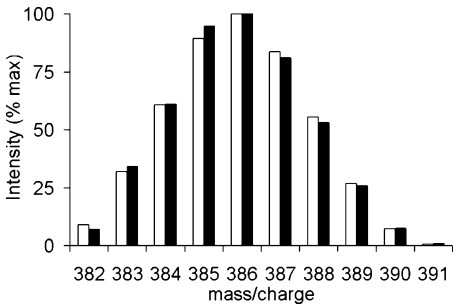

Figure 6. Experimental mass spectrum for the mixture of isotopomers of **12** shown as white bars, alongside the predicted mass spectrum for an intermolecular reaction pathway with a 1:4:6:4:1 ratio of nondeuterated through to tetradeuterated species shown as black bars. The best fit was obtained using a model with 52% H and 48% D.

(20) (a) Masselot, D.; Charmant, J. P. H.; Gallagher, T. *J. Am. Chem. Soc.* **2006**, *128*, 694−695. (b) Ma, S.; Gu, Z. *Angew. Chem., Int. Ed.* **2005**, *44*, 7512−7517. (c) Singh, A.; Sharp, P. R. *J. Am. Chem. Soc.* **2006**, *128*, 5998−5999. (d) Liu, Z.; Zhang, X.; Larock, R. C. *J. Am. Chem. Soc.* **2005**, *127*, 15716−15717. (e) Karig, G.; Moon, M.-T.; Thasana, N.; Gallagher, T. *Org. Lett.* **2002**, *4*, 3115−3118.
(21) (a) Campeau, L.-C.; Parisien, M.; Jean, A.; Fagnou, K. *J. Am. Chem. Soc.* **2006**, *128*, 581−590. (b) Garcia-Cuadrado, D.; Braga, A. A. C.; Maseras, F.; Echavarren, A. M. *J. Am. Chem. Soc.* **2006**, *128*, 1066−1067. (c) Bour, C.; Suffert, J. *Org. Lett.* **2005**, *7*, 653−656.
(22) (a) Miura, T.; Sasaki, T.; Nakazawa, H.; Murakami, M. *J. Am. Chem. Soc.* **2005**, *127*, 1390−1391. (b) Oguma, K.; Miura, M.; Satoh, T.; Nomura, M. *J. Am. Chem. Soc.* **2000**, *122*, 10464−10465. (c) Yamabe, H.; Mizuno, A.; Kusama, H.; Iwasawa, N. *J. Am. Chem. Soc.* **2005**, *127*, 3248−3249.
(23) (a) Davies, D. L.; Donald, S. M. A.; Macgregor, S. A. *J. Am. Chem. Soc.* **2005**, *127*, 13754−13755. (b) Mota, A. J.; Dedieu, A.; Bour, C.; Suffert, J. *J. Am. Chem. Soc.* **2005**, *127*, 7171−7182.
(24) Hughes, R. P. *Adv. Organomet. Chem.* **1990**, *31*, 183−267.

Scheme 5

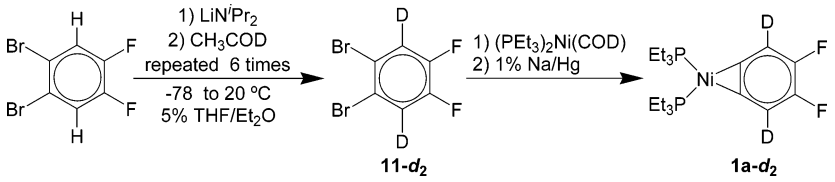

Scheme 6

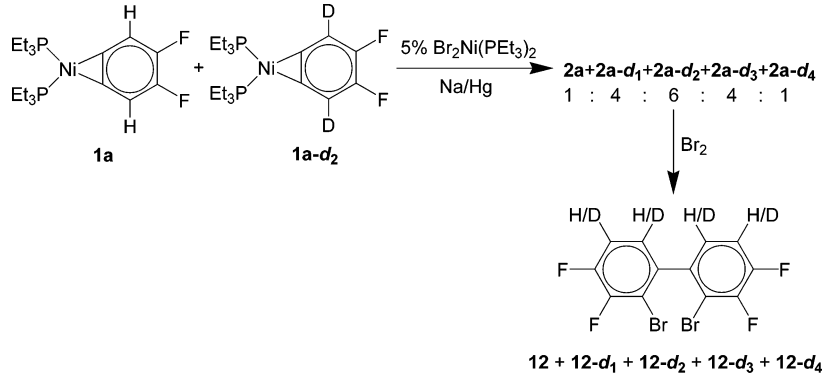

state molecular structure of the known compound $(PEt_3)_2Ni(\eta^2\text{-}C_6H_4C_6H_4)$ (**10**)[8] was determined by X-ray crystallography and is shown in Figure 5.

The geometry at the nickel center in **10** is intermediate between square planar and tetrahedral, as evidenced by the angle of 45.7° between the planes defined by P(1)−Ni(1)−P(1) and C(2)−Ni(1)−C(2). It is unlikely that strain in the biaryl chelate is the cause of this distortion; the C(1)−Ni(1)−C(1a) angle of 82.88(12)° is not particularly small compared to other Ni(II) complexes, and the C1−C2−C(2a) angle of 112.29(11)° is nearly identical to the corresponding angle in the structure of **2a**. Also, many complexes similar to **10**, where the chelating bis(diisopropylphosphino)ethane[6] or bis(dicyclohexylphosphino)ethane[25] ligands are used in lieu of triethylphosphine, are only slighted distorted from a planar geometry. Related examples where slightly distorted geometries occur at Ni(II) centers have been reported.[26] It seems that solely steric interactions between the triethylphosphine ligands and the hydrogen substitutuents of the biphenyldiyl in the 3,3′ positions cause the distortions evident in $(PEt_3)_2Ni(\eta^2\text{-}C_6H_4C_6H_4)$. This distortion may partly account for the relative apparent thermodynamic stability of the dinuclear Ni(I) complexes **2a**,**b** with respect to disproportionation into Ni(0) phosphine complexes and Ni(II) biarylyl complexes. The fact that **9a** was never identified as an intermediate in the isomerization of **1a** to **2a** and the failure to observe the conversion of **9a** to **2a** both provide evidence against the participation of mononuclear **9a** in this isomerization. These observations are consistent with the fact that the addition of PEt_3 inhibits the isomerization of **1a**. Attempts to generate a dinuclear Ni(I) complex from **10** by the addition of $Br_2Ni(PEt_3)_2$ and excess Na/Hg as a source of the $Ni(PEt_3)_2$ moiety failed; the Lewis acidic nature of the $Ni(PEt_3)_2$ moiety catalyzed the decomposition of **10** via the known C−C bond coupling pathway.[8] This provides evidence that the reversible interconversion of the dinuclear Ni(I) biarlylyl **7a** via heterolytic cleavage of the Ni−Ni bond to provide phosphine complexes of Ni(0) and a mononuclear Ni(II) biarylyl is unlikely under the conditions used to isomerize **1a** to **2a**.

Deuterium Labeling Studies. A deuterium labeling crossover experiment was performed to determine if the isomerization of **7a** to **2a** was intramolecular or involved intermolecular transfer of hydrogen. Multiple treatments of 1,2-dibromo-4,5-difluorobenzene with LiN^{i}Pr$_2$ followed by quenching with CH_3OD provided 1,2-dibromo-3,6-dideutero-4,5-difluorobenzene (**11-*d*$_2$**). This precursor could then be used to produce the dideuterated aryne **1a-*d*$_2$**, as shown in Scheme 5.

A solution consisting of approximately equal amounts of **1** and **1-*d*$_2$** in C_6D_6 was reacted with a catalytic amount of $Br_2Ni(PEt_3)_2$ over Na/Hg. When the reaction was complete, as monitored by ^{19}F NMR spectroscopy, the sample was reacted with Br_2 to replace the Ni centers with bromine atoms and filtered through a plug of alumina to produce $2,2'\text{-}Br_2\text{-}3,3',4,4'\text{-}F_4\text{-}C_{12}H_nD_{4-n}$ (**12-*d*$_n$**), where $n = 0$ to 4 as shown in Scheme 6.

The mass spectrum of the resultant biaryl isotopomers, **12-*d*$_n$**, is shown in Figure 6, alongside the spectrum predicted for an intermolecular scrambling of H/D labels. For an equimolar mixture of **1a** and **1a-*d*$_2$**, a mechanism that occurs with intermolecular exchange of the hydrogen/deuterium atom of the activated C−H/C−D bond should result in a 1:4:6:4:1 ratio of isotopomers that contain 0−4 deuterium atoms. The data do not fit the modeled spectrum for intramolecular transfer, which should produce a 1:0:2:0:1 ratio of isotopomers. They are also poorly fit by the modeled spectrum for a 1:2:2:2:1 ratio of isotopomers predicted if one of the two hydrogen/deuterium atoms was transferred intramolecularly and the other intermolecularly. A similar experiment performed in C_6D_6 with **1a** produced only $2,2'\text{-}Br_2\text{-}3,3',4,4'\text{-}F_4\text{-}C_{12}H_4$, which excludes the involvement of the solvent in these reactions.

By following the course of the reaction by ^{19}F NMR, it was possible to determine that there is not a large kinetic isotope effect in the rate of activation of the C−H bonds over the C−D bonds. The fluorine atoms ortho to deuterium substituents on

(25) Bennett, M. A.; Kopp, M. R.; Wenger, E.; Willis, A. C. *J. Organomet. Chem.* **2003**, *667*, 8−15.
(26) Jones, G. D.; Anderson, T. J.; Chang, N.; Brandon, R. J.; Ong, G. L.; Vicic, D. A. *Organometallics* **2004**, *23*, 3071−3074.

Table 1. X-ray Crystallographic Data and Structure Refinement Parameters for Complexes **4**, **6**, **7b**, and **10**

	4	6	7b	10
empirical formula	$C_{18}H_{33}F_{12}NiP_2$	$C_{36}H_{51}F_6NiP_3$	$C_{30}H_{52}F_4Ni_2P_4$	$C_{24}H_{38}NiP_2$
formula weight	642.89	866.81	730.02	447.19
T (K)	173(2)	223(2)	173(2)	173(2)
crystal system	monoclinic	monoclinic	monoclinic	tetragonal
space group	Pn	*P*2(1)/*n*	*C*2/*c*	*I*4(1)/*a*
a, Å	8.9858(15)	12.420(3)	19.576(2)	11.0586(19)
b, Å	12.415(2)	14.719(3)	28.862(3)	11.0586(19)
c, Å	10.8491(18)	21.426(5)	13.9109(15)	38.711(13)
α, deg	90	90	90	90
β, deg	95.168(2)	95.076(4)	117.1080(10)	90
γ, deg	90	90	90	90
V, Å^3	1205.4(3)	3901.8(15)	6996.3(13)	4734(2)
Z	2	4	8	8
μ (mm^{-1})	3.506	1.609	1.299	0.961
total reflns	13221	37187	39037	26292
No. unique; R_{int}	5356; 0.029	8938; 0.026	7946; 0.055	2827; 0.052
residuals: R1, wR2	0.045, 0.098	0.054, 0.136	0.073, 0.124	0.046, 0.092

the aromatic rings all exhibit an easily observable isotopic chemical shift of approximately −0.3 ppm compared to their hydrogen-substituted analogues, and thus the ratio of the integrals of these peaks can be used to estimate if rings bearing C−H bonds are activated faster than the rings bearing C−D bonds. Throughout the course of the reaction, the ratio of peak integrals for F atoms ortho to H versus F atoms ortho to D is approximately 1 for the reactants, intermediates, and products, although this technique is not accurate enough to determine the very small inverse kinetic isotope effects that are sometimes observed for C−H bond activations.[27]

The intermolecular scrambling observed implies that the rate constants shown in Scheme 4 represent processes with at least two elementary steps and that nickel hydride complexes may exist as intermediates in these reactions, whether the mechanism involves the oxidative addition of C−H bonds or electrophilic C−H bond activation. Ni(0) phosphine complexes could potentially act as bases to form Ni(II) hydrides. All attempts to identify peaks in the ^{1}H NMR spectra that could be assigned as Ni hydrides during the conversion of **1a** to **2a** failed; species such as the dinuclear bis(phosphine) Ni(I) hydrides[28] or cationic mononuclear Ni(II) hydrides[29] should exhibit distinctive shifts and couplings to phosphorus nuclei but would be expected to be present in very low concentrations. Mechanisms involving electrophilic activation that produce acidic intermediates are unlikely, because any strongly acidic protons in these systems should be reduced by sodium when these reactions are performed using **1a** and catalytic $Br_2Ni(PEt_3)_2$ over Na/Hg.

Conclusions

Both the identification of intermediates and the relative rate at which they are formed and consumed have allowed for a detailed understanding of the C−C bond forming and C−H bond activation steps that isomerize the aryne complex **1a** into the biarylyl complex **2b**. This study demonstrates that the initial step involves C−C bond formation, depicted as mechanism B in Scheme 1, and is due to the behavior of the $Ni(PEt_3)_2$ moiety as a Lewis acid that can abstract PEt_3 from **1a**. The proposed mechanism of C−H bond rearrangement in these biarylyl complexes utilizes 1,4-shifts, which have been observed in biphenyl and related aromatic complexes of Pt(II) and Pd(II),[20] some of which require high temperatures. Facile 1,4- and 1,5-shifts have also been reported in a variety of systems that contain Pd(II)[21] and Rh(I).[22] None of these examples utilize first row metals, such as Ni, and they also all differ in that they involve d^8 metal centers. A deuterium labeling crossover experiment demonstrates the intermolecular scrambling of hydrogen and deuterium labels, which indicates a true C−H bond-breaking step must occur; the low barrier to this rearrangement cannot be due to a concerted mechanism. The observation of 2 equiv of intermediate **8a** for every equivalent of **2a** early in the reaction implies that **8a** is not directly on the reaction pathway and implies that both complexes share a common intermediate. The ability of Ni(I) complexes to undergo these rearrangements at room temperature holds promise for increasing the scope of these C−H bond activations to a variety of aromatic systems.

Experimental Section

General Procedures. Unless otherwise stated, all manipulations were performed under an inert atmosphere of nitrogen using either standard Schlenk techniques or an MBraun glove box. Dry, oxygen-free solvents were employed throughout. Anhydrous pentane was purchased from Aldrich, sparged with dinitrogen, and passed through activated alumina under a positive pressure of nitrogen gas and further deoxygenated using Ridox catalyst columns.[30] Deuterated benzene was dried by heating at reflux with sodium/potassium alloy in a sealed vessel under partial pressure, then trap-to-trap distilled, and freeze−pump−thaw degassed three times. Deuterated toluene was purified in an analogous manner by being heated at reflux over Na. NMR spectra were recorded on Bruker AMX (300 MHz) or Bruker AMX (500 MHz) spectrometer. All chemical shifts are reported in parts per million (ppm), and all coupling constants are in hertz (Hz). For ^{19}F{^{1}H} NMR spectra, trifluoroacetic acid was used as the external reference at 0.00 ppm. ^{1}H NMR spectra were referenced to residual protons (C_6D_5H, 7.15; C_7D_7H, δ 2.09) with respect to tetramethylsilane at δ 0.00. ^{31}P{^{1}H} NMR spectra were referenced to external 85% H_3PO_4 at δ 0.0. ^{13}C{^{1}H} spectra were referenced relative to solvent resonances (C_6D_6, δ 128.0; C_7D_8, δ 20.4). UV/visible spectra were obtained on a Varian Carey 50 spectrophotometer. Elemental analyses were performed by the Centre

(27) (a) Jones, W. D. *Acc. Chem. Res.* **2003**, *36*, 140−146. (b) Churchill, D. G.; Janak, K. E.; Wittenberg, J. S.; Parkin, G. *J. Am. Chem. Soc.* **2003**, *125*, 1403−1420.
(28) (a) Bach, I.; Goddard, R.; Kopiske, C.; Seevogel, K.; Poerschke, K.-R. *Organometallics* **1999**, *18*, 10−20. (b) Jonas, K.; Wilke, G. *Angew. Chem., Int. Ed.* **1970**, *9*, 312−313. (c) Vicic, D. A.; Jones, W. D. *J. Am. Chem. Soc.* **1997**, *119*, 10855−10856.
(29) Schunn, R. A. *Inorg. Chem.* **1976**, *15*, 208−212.
(30) Pangborn, A. B.; Giardello, M. A.; Grubbs, R. H.; Rosen, R. K.; Timmers, F. J. *Organometallics* **1996**, *15*, 1518−1520.

for Catalysis and Materials Research, Windsor, Ontario, Canada. The compounds $(Et_3P)_2NiBr(2\text{-}Br\text{-}4,5\text{-}F_2\text{-}C_6H_2)$,[11] $Ni(PEt_3)_4$,[31] and 1-F-2,3-$I_2C\text{-}C_6H_3$[17] were prepared by literature procedures. The complex $Br_2Ni(PEt_3)_2$ was prepared by the addition of PEt_3 to commercially available $(DME)NiBr_2$ followed by recrystallization from pentane. The compounds PEt_3, $B(C_6F_5)_3$, Na, and Hg were purchased from Aldrich. The compound $B(C_6F_5)_3$ was sublimed prior to use.

Synthesis of $(PEt_3)_4Ni_2(\mu\text{-}\eta^1\text{:}\eta^1\text{-}3,3',4,4'\text{-}F_4\text{-}C_{12}H_4)$ (2a). To a stirred solution of $NiBr(2\text{-}Br\text{-}4,5\text{-}F_2C_6H_2)(PEt_3)_2$ (0.5 g, 0.88 mmol) in 20 mL of pentane over excess 1% Na/Hg amalgam (40 g) was added a solution of $Br_2Ni(PEt_3)_2$ (0.1 g, 0.22 mmol) in 15 mL of pentane. The solution was then stirred slowly for 20 h. The solution was then filtered through Celite, and the volume was reduced to ca. 20 mL. The solution was cooled to −40 °C, upon which dark brown crystals of $(PEt_3)_4Ni_2(C_6H_2F_2)_2$ were obtained (0.22 g, 60% yield). ^{1}H NMR (C_6D_6, 20 °C, 500 MHz): δ 1.05 (br, 36H, CH_3), 1.90 (br, 24H, CH_2), 6.55 (m, 4H). ^{1}H NMR (C_6D_6, −60 °C, 500 MHz, aromatic region): δ 6.44 (ddd, 2H, $^3J_{HH} = 8.0$, $^4J_{HF} = 4.0$, $^5J_{HF} = 0.7$ Hz), 6.64 (ddd, $^3J_{HH} = 8.0$ Hz, $^4J_{H(a)F(b)} = 7.3$ Hz, $^4J_{H(a)F(a)} = 10.2$ Hz). ^{31}P{^{1}H} NMR (C_6D_6, 20 °C, 202.47 MHz): δ 8.8 (br s), −3.8 (br s). ^{31}P{^{1}H} NMR (C_6D_6, −60 °C, 202.47 MHz): δ −3.8 (vt, $J_{PP} = 5.4$ Hz), 8.8 (vtdd, $J_{PP} = 5.4$ Hz, $J_{FP} = 7.1$, 11.3 Hz). ^{19}F NMR (C_6D_6, 20 °C, 282.48 MHz): δ −34.3 (dddd, $^4J_{H(a)F(a)} = 10.2$ Hz, $^4J_{H(b)F(a)} = 4.0$ Hz, $^3J_{FF} = 35.6$ Hz, $J_{FP} = 6.0$ Hz), −71.1 (ddd, $J_{FP} = 11.5$ Hz, $J_{H(a)F(b)} = 7.3$ Hz, $^3J_{FF} = 35.6$ Hz). ^{13}C{^{1}H} NMR (C_6D_6, 298 K, 75.50 MHz): δ 8.2 and 9.5 (br, *C*H_3), 17.1 and 21.5 (br, *C*H_2), 109.9 (d, $^2J_{CF} = 19.8$ Hz), 114.23 (s, ipso-C), 150.5 (dd, $^1J_{CF} = 244.3$ Hz, $^2J_{CF} = 22.0$ Hz), 151.5 (d, $^2J_{CF} = 17.6$ Hz), 155.7 (dd, $^1J_{CF} = 226.1$ Hz, $^2J_{CF} = 14.7$ Hz), 155.9 (s, ipso-C). Anal. Calcd: C, 53.11; H, 7.92. Found: C, 52.67; H, 7.81. UV/vis: ϵ = 72 000 L mol^{-1} cm^{-1}. $\lambda_{max} = 428$ nm.

Synthesis of $[(PEt_3)_2Ni]_2(\mu\text{-}\eta^2\text{:}\eta^2\text{-}C_6H_2F_2)$ (3). To a stirred solution of $Ni(\eta_2\text{-}C_6H_2F_2)(PEt_3)_2$ (80 mg, 0.197 mmol) in 15 mL of pentane over excess 1% Na/Hg amalgam (50 g) was added dropwise, over 1 h, a dilute solution of $Br_2Ni(PEt_3)_2$ (89 mg, 0.197 mmol) in 25 mL of pentane. The solution was then stirred for 20 min before being filtered through Celite, and the solvent was reduced to ca. 20 mL. The solution was then cooled to −40 °C, and pale orange crystals of $Ni_2(\mu\text{-}\eta^2\text{:}\eta^2\text{-}C_6H_2F_2)(PEt_3)_2$ were obtained (60 mg, 43% yield). ^{1}H NMR (C_6D_6, 20 °C, 300 MHz): δ 0.91 (m, 18H, C*H*$_3$), 1.42 (m, 12H, C*H*$_2$), 7.33 (t, 2H, $^3J_{HF} = 7.3$ Hz). ^{31}P{^{1}H} NMR (C_6D_6, 20 °C, 121.54 MHz): δ 14.8 (s). ^{19}F NMR (C_6D_6, 20 °C, 282.46 MHz): δ −74.0 (m). Anal. Calcd: C, 51.32; H, 8.90. Found: C, 51.68; H, 8.70.

Synthesis of $NiI(3\text{-}F\text{-}2\text{-}I\text{-}C_6H_3)(PEt_3)_2$ (4). A suspension of $Ni(COD)_2$ (0.55 g, 0.002 mol) in 25 mL of pentane was cooled to 0 °C. A solution of PEt_3 (0.59 g, 0.005 mol) was added dropwise to the solution and stirred for 5 min. A solution of 2,3-diiodofluorobenzene (1.02 g, 0.003 mol) in 25 mL of pentane was then added. The mixture was stirred for 10 min at 0 °C and then for 4 h at room temperature. The solvent was then removed under vacuum, and the residue was extracted with pentane and filtered through Celite. The solution was then placed in the freezer at −40 °C. Dark yellow crystals of $NiI(2\text{-}I\text{-}3\text{-}FC_6H_3)(PEt_3)_2$ were isolated (0.27 g, 30% yield). ^{1}H NMR (C_6D_6, 298 K, 300 MHz): δ 0.96 (m, 18H), 1.52 (m, 12H), 6.44 (dd, 1H, $J_{HF} = 8.8$ Hz, $J_{HH} = 7.6$ Hz), 6.65 (m, 2H). ^{31}P{^{1}H} NMR (C_6D_6, 298 K, 202.47 MHz): δ 9.9 (s). ^{19}F NMR (C_6D_6, 298 K, 282.48 MHz): δ −13.2 (d, $J_{HF} = 8.8$ Hz). Anal. Calcd for $C_{18}H_{33}I_2FP_2Ni$: C, 33.63; H, 5.17. Found: C, 33.78; H, 5.24.

Synthesis of $Ni(\eta^2\text{-}3\text{-}F\text{-}C_6H_3)(PEt_3)_2$ (5). A solution of $NiI(2\text{-}I\text{-}3\text{-}FC_6H_3)(PEt_3)_2$ (0.10 g, 0.26 mmol) in 25 mL of pentane was stirred over excess 1% Na/Hg (40 g) for 1 h. The solution was then filtered through Celite. The solvent was then removed under vacuum, leaving a dark yellow oil that freezes below 0 °C (0.037 g, 62% yield). ^{1}H NMR (C_6D_6, 298 K, 300 MHz): δ 0.97 (overlapping br m, 18H, CH_3), 1.46 and 1.56 (br m, 12H, CH_2), 6.93 (dd, 1H, $J_{HF} = 3.3$ Hz, $J_{HH} =$ 6.7 Hz, aromatic 6-H), 7.18 (ddd, 1H, $J_{HF} = 3.3$ Hz, $J_{HH} = 6.7$ Hz, $J_{HH} = 7.4$ Hz, aromatic-5-H), 7.41 (dd, 1H, $J_{HF} = 6.3$ Hz, $J_{HH} = 7.4$ Hz, aromatic-4-H). ^{31}P{^{1}H} NMR (C_6D_6, 298 K, 202.47 MHz): δ 29.7 (br s), 27.1 (br s). ^{19}F NMR (C_6D_6, 298 K, 282.48 MHz): δ −28.4 (ddd, $J_{HF} = 6.3$ Hz, $J_{HF} = 3.3$ Hz, $J_{HF} = 3.3$ Hz). ^{13}C{^{1}H} NMR (C_6D_6, 298 K, 125.27 MHz): δ 9.0 and 9.3 (br, PCH_2*Me*), 20.0 and 20.7 (br, *PCH*$_2$), 113.0 (d, $J = 32.5$ Hz), 118.0 (s), 129.4 (d, $J = 97$ Hz), 130.2 (s), 153.9 (br d, $J = 10$ Hz), 163.1 (d, $^1J_{CF} = 254.8$ Hz).

Synthesis of $(PEt_3)_3Ni_3(\mu_3\text{-}4,5\text{-}F_2C_6H_2)(\mu_3\text{-}4,5\text{-}F_2C_6H_2\text{-}4',5'\text{-}F_2C_6H_2)$ (6). To a stirred solution of $Ni(\eta^2\text{-}C_6H_2F_2)(PEt_3)_2$ (0.65 g, 0.0016 mol) in 25 mL of pentane was added dropwise a solution of tris(pentafluorophenyl)borane ($B(C_6F_5)_3$) (0.82 g, 0.0016 mol) in 15 mL of pentane. The resulting brown solution was stirred for 15 min and then filtered to remove the white precipitate. The solvent was then reduced to half volume, and the product was recrystallized at −40 °C to yield $(PEt_3)_3Ni_3(\eta^2\text{-}C_6H_2F_2)(\eta^2\text{-}C_6H_2F\text{-}C_6H_2F_2)$ as dark brown crystals in a 31% yield. ^{1}H NMR (C_6D_6, 298 K, 500 MHz): δ 0.66 (br m, 27 H, CH_3), 1.00(br m, 18 H, CH_2), 6.97(dd, 2 H, $J_{HF} = 12.3$ Hz, $J_{HF} = 7.2$ Hz), 7.34 (vt, 2 H, $J_{HF} = 9.5$ Hz), 7.79(dd, 2 H, $J_{HF} = 10.6$ Hz, $J_{HF} = 8.8$ Hz). ^{31}P{^{1}H} NMR (C_6D_6, 298 K, 202.47 MHz): δ 13.2 (br, 2P), 5.1 (br, 1P). ^{13}C{^{1}H} NMR (C_6D_6, 298 K, 75.50 MHz): δ 108.25 (d, $^2J_{CF} = 12.6$), 111.8 (d, $^2J_{CF} = 18.9$ Hz), 131.0 (d, $^2J_{CF} =$ 12.6 Hz), 135.8 (s, *ipso* C), 146.1 (dd, $^1J_{CF} = 251.5$ Hz, $^2J_{CF} = 18.9$ Hz), 148.4 (dd, $^1J_{CF} = 213.8$, $^2J_{CF} = 12.6$), 149.1 (dd, $^1J_{CF} = 232.6$, $^2J_{CF} = 12.6$), 151.4 (s, ipso C), 168.1 (s, ipso C). ^{19}F NMR (C_6D_6, 298 K, 282.48 MHz): δ −69.1 (ddd, $^3J_{FF} = 19.9$ Hz, $J_{HF} = 12.3$ Hz, $J_{HF} = 8.8$ Hz), −66.5 (vt, $J_{HF} = 9.5$ Hz), −61.6 (ddd, $^3J_{FF} = 19.9$ Hz, $J_{HF} = 10.6$ Hz, $J_{HF} = 7.2$ Hz). Anal. Calcd for $C_{39}H_{77}F_6Ni_3P_3$: C, 49.88; H, 5.93. Found: C, 49.56; H, 5.91.

Synthesis of $[(PEt_3)_2Ni]_2(\mu\text{-}\eta^2\text{:}\eta^2\text{-}4,5\text{-}F_2C_6H_2\text{-}4',5'\text{-}F_2C_6H_2)$ (7a). To a solution of **6** (0.12 g, 0.154 mmol) in 20 mL of pentane was added PEt_3 (0.06 mL, 0.406 mmol, 2.6 equiv) and stirred for 5 min. The mixture was then reduced to ca. 10 mL and placed in the freezer at −40 °C. The products separated as a dark oily product. ^{1}H, ^{31}P-{^{1}H}, and ^{19}F NMR data were used to identify $(PEt_3)_4Ni_2(\eta^2\text{-}C_6H_2\text{-}3,4\text{-}F_2)_2$ (**1a**) and a second product assigned as $[(PEt_3)_2Ni]_2(4,5\text{-}F_2C_6H_2\text{-}4',5'\text{-}F_2C_6H_2)$ (**7a**). ^{1}H NMR (C_6D_6, 298 K, 300 MHz): δ 1.09 (br, 36H, CH_3), 1.86 (br, 24H, CH_2), 6.58 (dd, $J_{HF} = 7.6$, 11.9 Hz, aromatic), 6.77 (dd, $J_{HF} = 9.4$, 11.2 Hz, aromatic). ^{31}P{^{1}H} NMR (C_6D_6, 20 °C, 202.47 MHz): δ 8.1 (br), −6.6 (br). ^{19}F NMR (C_6D_6, 298 K, 282.48 MHz): δ −72.7 (m, $J_{HF} = 11.9$, 9.4 Hz, $J_{FF} = 20.0$ Hz), −73.0 $J_{HF} =$ 11.2, 7.6 Hz, $J_{FF} = 20.0$ Hz).

Synthesis of $[(PEt_3)(PMe_3)Ni]_2(\mu\text{-}\eta^1\text{:}\eta^1\text{-}4,5\text{-}F_2C_6H_2\text{-}4',5'\text{-}F_2C_6H_2)$ (7b). To a solution of **6** (0.111 g, 0.142 mmol) in 15 mL of pentane was added PMe_3 (0.044 mL, 0.43 mmol). The solution was stirred for 5 min and then cooled to −40 °C. The first compound to precipitate out of solution was $Ni(\eta^2\text{-}C_6H_2F_2)(PMe_3)(PEt_3)$, **1b**, as an orange solid. This was filtered off, and the remaining solution was concentrated and cooled to −40 °C. Brown crystals of $(PEt_3)_2(PMe_3)_2Ni_2(\eta^2\text{-}C_6H_2\text{-}3,4\text{-}F_2)_2$ were isolated (0.03 g, 32% yield). ^{1}H NMR (C_6D_6, 298 K, 300 MHz): δ 1.03 (m, 18H, C*H*$_3$, PEt_3), 1.15 (d, 18H, C*H*$_3$ of PMe_3), 1.38 (m, 12H, PC*H*$_2$), 6.57 (dd, $J = 7.1$ Hz, $J = 11.6$ Hz, 2H, aromatic), 6.70 (dd, 2H). ^{31}P{^{1}H} NMR (C_6D_6, 298 K, 202.47 MHz): δ −0.3 (vt, $J = 10.3$ Hz, Ni-*P*Et_3), −21.2 (vt, $J = 10.3$ Hz, Ni-*P*Me_3). ^{19}F NMR (C_6D_6, 298 K, 282.48 MHz): δ −73.0 (m), −73.6 (m). Anal. Calcd for $C_{30}H_{52}F_4Ni_2P_4$: C, 49.36; H, 7.18. Found: C, 49.56; H, 7.32.

Complex 9a. To a solution of **6** (0.14 g, 0.179 mmol) in 15 mL of pentane was added PEt_3 (0.20 mL g, 1.35 mmol) and stirred. The mixture was then reduced to ca. 10 mL and placed in the freezer at −40 °C. The products separated as a pale brown oil. ^{1}H, ^{31}P{^{1}H}, and ^{19}F NMR data were used to identify excess PEt_3, $Ni(PEt_3)_4$, $(PEt_3)_4Ni_2(\eta^2\text{-}C_6H_2\text{-}3,4\text{-}F_2)_2$ (**1**), and a product assigned tentatively as $[(PEt_3)_2Ni](4,5\text{-}F_2C_6H_2\text{-}4',5'\text{-}F_2C_6H_2)$ (**9a**); complex **9a** is thermally unstable in the absence of Pet_3 and could not be isolated pure. ^{1}H NMR (C_6D_6, 298 K, 300 MHz): δ 6.79 (dd, 2H, $J_{HF} = 8.6$ Hz, $J_{HF} = 10.7$ Hz, aromatic *H*), 6.81 (dd, 2H, $J_{HF} = 7.5$ Hz, $J_{HF} = 11.8$ Hz, aromatic *H*).

(31) Cundy, C. S. *J. Organomet. Chem.* **1974**, *69*, 305−310.

$^{31}P\{^1H\}$ NMR (C_6D_6, 298 K, 202.47 MHz): δ 3.6 (br). ^{19}F NMR (C_6D_6, 298 K, 282.48 MHz): δ −67.7 (ddd, J_{FF} = 20.3 Hz, J_{HF} = 11.8 Hz, $^4J_{HF}$ = 8.6 Hz), −65.4 (dddd, J_{FF} = 20.3 Hz, J_{HF} = 10.7 Hz, $^4J_{HF}$ = 7.5 Hz, J_{PF} = 2.3 Hz).

Synthesis of 1,2-Dibromo-3,6-dideutero-4,5-difluorobenzene (11-*d*$_2$). To a stirred solution of 1,2-dibromo-4,5-difluorobenzene (18.4 mmol, 5 g) in 25 mL of 5% THF in Et_2O at −78 °C was added dropwise a suspension of lithiumdiisopropylamide (18.4 mmol, 1.97 g, 1 equiv) in 20 mL of 5% THF in Et_2O. The solution was stirred for 20 min. $DOCH_3$ (18.4 mmol, 0.608 g, 1 equiv) was added to the mixture dropwise. The solution was then allowed to slowly warm to room temperature over 1.5 h, at which point a sample was taken to monitor progress. This process was repeated for a total of six additions of LDA and $DOCH_3$. The solvent was removed under vacuum, and the residue was extracted with four portions of ca. 50 mL of pentane. The pentane was removed under vacuum, which afforded a yellow oil. The oil was cooled to 0 °C to provide colorless crystals of 1,2-Br_2-4,5-$F_2C_6D_2$ (1.0 g, 20% yield). ^{19}F NMR (C_6D_6, 300 K, 282.48 MHz): δ −58.5 (virtual pentet, J = 1.3 Hz). Anal. Calcd for $C_6F_2D_2$: C, 26.31; D, 1.47. Found: C, 26.55; D, 1.53.

Synthesis of NiBr(2-Br-4,5-$F_2C_6D_2$)(PEt_3)$_2$. A stirred suspension of $Ni(COD)_2$ (2.6 mmol, 0.715 g) in 20 mL of pentane was cooled to 0 °C, and PEt_3 (5.1 mmol, 0.604 g, 2 equiv) was added followed by a solution of 1,2-dibromo-3,6-dideutero-4,5-difluorobenzene (2.6 mmol, 0.7 g) in ca. 15 mL of pentane. The mixture was stirred for 10 min at 0 °C and then for 4 h at room temperature. The solvent was removed under vacuum. The residue was extracted with 50 mL of pentane and filtered through Celite. The solvent was then reduced to 25 mL and cooled to −40 °C to provide NiBr(2-Br-4,5-$F_2C_6D_2$)(PEt_3)$_2$ as a yellow solid from pentane at (0.752 g, 51% yield). ^1H NMR (C_6D_6, 300 K, 300 MHz): δ 0.91 (m, 18H, C*H*$_3$), 1.32 (m, 12H, C*H*$_2$). $^{31}P\{^1H\}$ NMR (C_6D_6, 300 K, 121.54 MHz): δ 10.6 (s). ^{19}F NMR (C_6D_6, 300 K, 282.48 MHz): δ −67.2 (dt, $^3J_{FF}$ = 20.4 Hz, J_{FD} = 1.6 Hz), −64.7 (dt, $^3J_{FF}$ = 20.4 Hz, J_{FD} = 1.6 Hz). Anal. Calcd for $C_{18}H_{30}D_2Br_2F_2P_2Ni$: C, 38.00; D, 6.02. Found: C, 38.04; D, 5.99.

Synthesis of (PEt_3)$_2$Ni(η^2-C_6D_2-4,5-F_2), (1a-*d*$_2$). The synthesis of **1a-*d*$_2$** was performed in an analogous manner to the known literature procedure for the preparation of **1a**. $^{31}P\{^1H\}$ NMR (C_6D_6, 298 K, 202.47 MHz): δ 29.5 (br). ^{19}F NMR (C_6D_6, 300 K, 282.48 MHz): δ −60.3 (br).

Synthesis of [(PEt_3)$_2$Ni]$_2$(μ-η^1:η^1-3,4-$F_2C_6D_2$-3′,4′-$F_2C_6D_2$), (2a-*d*$_4$). To a solution of **1a-*d*$_2$** (0.04 g, 0.098 mmol) in 2 mL of pentane was added (PEt_3)$_2$$NiBr_2$ (0.004 g, 0.0088 mmol, 0.09 equiv) and 0.5 g of 1% Na/Hg. The solution was stirred for 24 h. No aromatic proton resonances associated with the biarylyl complex were observed in the ^1H NMR spectrum. ^{19}F NMR (C_6D_6, 300 K, 282.48 MHz): δ −34.3 (br d, $^3J_{FF}$ = 33.8 Hz), −71.4 (br d, $^3J_{FF}$ = 33.8 Hz).

Deuterium Labeling Crossover Study. Approximately equal masses of **1a** and **1a-*d*$_2$** (∼10 mg) were dissolved in C_6D_6. The solution was then stirred with 1 mg of $Br_2Ni(PEt_3)_2$ and 0.5 g of 1% Na/Hg, and the reaction was monitored by ^{19}F NMR spectroscopy. When the conversion to **2a-*d*$_n$** (n = 1−4) was complete, the solution was quenched by the direct addition of Br_2, and the solution was passed through a plug of acidic alumina and analyzed by ^{19}F NMR and GC/MS. ^{19}F NMR ($CDCl_3$, 300 K, 282.48 MHz): δ −48.2 (overlapping multiplets), −55.3 (overlapping m, $^3J_{FF}$ = 22.0 Hz, $^3J_{HF}$ = 9.3 Hz, $^4J_{HF}$ = 5.0 Hz, 4,5-H_2 isomer; $^3J_{FF}$ = 22.0 Hz, $^3J_{HF}$ = 9.3 Hz, 4-H-5-D isomer), −55.6 (overlapping m, $^3J_{FF}$ = 22.0 Hz, 4,5-D_2 and 4-D-5-H isomer). GC/MS (mass, intensity): 382, 6.99; 383, 34.15; 384, 60.97; 385, 94.70; 386, 99.97; 387, 81.06; 388, 53.07; 389, 25.79, 390, 7.40; 391, 0.786.

An analogous procedure using only **1a** produced 2,2′-dibromo-3,3′,4,4′-tetrafluorobiphenyl. ^{19}F NMR ($CDCl_3$, 300 K, 282.48 MHz): δ −48.2 (ddd, $^3J_{FF}$ = 21.9 Hz, $^4J_{HF}$ = 7.4 Hz, $^5J_{HF}$ = 2 Hz), −55.5 (dd, $^3J_{FF}$ = 21.9 Hz, $^3J_{HF}$ = 9.4 Hz, $^4J_{HF}$ = 5.1 Hz).

X-ray Crystallography. The X-ray structures were obtained at low temperature, with the crystal covered in Paratone and placed rapidly into the cold N_2 stream of the Kryo-Flex low-temperature device. The data were collected using the SMART[32] software on a Bruker APEX CCD diffractometer using a graphite monochromator with Mo Kα radiation (λ = 0.71073 Å). A hemisphere of data was collected using a counting time of 10−30 s per frame. Details of crystal data, data collection, and structure refinement are listed in Table 1. Data reductions were performed using the SAINT[33] software, and the data were corrected for absorption using SADABS.[34] The structures were solved by direct methods using SIR97[35] and refined by full-matrix least-squares on F^2 with anisotropic displacement parameters for the non-hydrogen atoms using SHELXL-97[36] and the WinGX[37] software package, and thermal ellipsoid plots were produced using ORTEP32.[38] Complex **6** features disorder of some of the ethyl substituents on the PEt_3 donors; the carbon atoms were treated as 2-fold disordered and refined isotropically. The hydrogen atoms associated with the disordered fragments were omitted from the model.

Calculations. Ab initio DFT calculations were performed using the hybrid functional B3LYP[39] method with the Gaussian 03 package.[40] The basis functions used were the 6-311+G(d) set, provided in the Gaussian 03 program.

Acknowledgment. Acknowledgment is made to the National Sciences and Engineering Council (NSERC) of Canada and the Ontario Research and Development Challenge Fund (ORDCF) for their financial support, and to Paul R. Sharp for his helpful comments and for providing a preprint of a relevant publication.

Supporting Information Available: Full details of ref 40; crystallographic information in CIF format for **4**, **6**, **7b**, and **10**; ORTEP depiction of the solid-state molecular structure of **4**, as determined by X-ray crystallography; optimized coordinates and energies for DFT calculations. This material is available free of charge via the Internet at http://pubs.acs.org.

JA067112W

(32) *SMART*, Molecular analysis research tool; Bruker AXS: Madison, WI, 2001.
(33) *SAINTPlus*, Data reduction and correction program; Bruker AXS: Madison, WI, 2001.
(34) *SADABS*, An empirical absorption correction program; Bruker AXS: Madison, WI, 2001.
(35) Altomare, A.; Burla, M. C.; Camalli, M.; Cascarano, G. L.; Giacovazzo, C.; Guagliardi, A.; Moliterni, A. G. G.; Polidori, G.; Spagna, R. *J. Appl. Crystallogr.* **1999**, *32*, 115−119.
(36) Sheldrick, G. M. *SHELXL-97*; University of Göttingen: Göttingen, Germany, 1997.
(37) Farrugia, L. J. *J. Appl. Crystallogr.* **1999**, *32*, 837−838.
(38) Farrugia, L. J. *J. Appl. Crystallogr.* **1997**, *30*, 565.
(39) Becke, A. D. *J. Chem. Phys.* **1993**, *98*, 5648−5652.
(40) Frisch, M. J.; et al. *Gaussian 03*, revision C.01; Gaussian, Inc.: Wallingford, CT, 2004.